ACS OMEGA

Open Access

http://pubs.acs.org/journal/acsodf

Article

Scalable Synthesis of the Key Fexuprazan Intermediate and Investigation of a Reaction Mechanism

Ting Wang, Yueting Hua, Fangbo Deng, Rui Wen, Haoyu Zhang, Chunshi Li, Yang Liu,* and Maosheng Cheng*

Cite This: *ACS Omega* 2024, 9, 37942−37952

Read Online

ACCESS | Metrics & More | Article Recommendations | Supporting Information

ABSTRACT: A three-step method for the synthesis of methyl 5-(2,4-difluorophenyl)-4-methoxy-1*H*-pyrrole-3-carboxylate **1**, a key intermediate of fexuprazan, is reported in this paper. Using low-priced sodium *p*-tolylsulfinate as the starting material, compound **28** was obtained with a 96.8% yield in the first step by optimizing the experimental parameters with a Box−Behnken experimental design. Subsequently, isonitrile compound **29** was obtained by dehydration. Finally, impurities **31** and **32** in the last step of the reaction were identified and converted into target product **1** by a one-pot method, which significantly improves the utilization of atoms. Key intermediate **1** was obtained via a three-step process with a yield of 68−70% and purity that exceeded 99%. In addition, the mechanism of the cyclization reaction was proposed. This method has potential for industrial production because the raw materials are inexpensive, the procedure is simple, and a high yield is obtained.

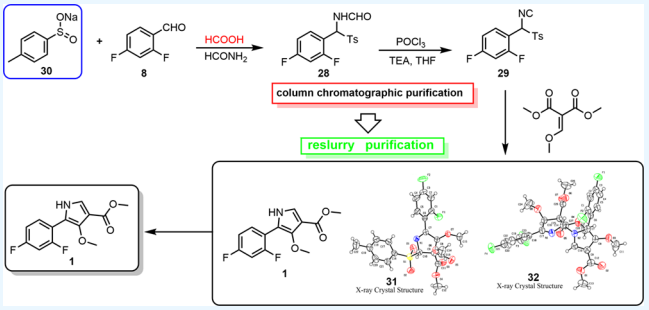

1. INTRODUCTION

Fexuprazan (DWP14012), a novel potassium-competitive acid blocker (P-CAB) developed by Daewoong Pharmaceutical Co., Ltd. (Seoul, Korea), was approved in Korea in 2022 for the treatment of gastroesophageal reflux disease (GERD). The clinical management of GERD primarily involves treatments that neutralize or reduce gastric acid, and proton pump inhibitors (PPIs) are the most commonly prescribed medications. In contrast to irreversible PPIs, fexuprazan is acid-stable and inhibits H^+, K^+-ATPase in a competitive and reversible manner, which results in a faster onset and a longer duration of gastric acid suppression. According to the results of a phase III, randomized, and double-blind trial, the healing rate of erosive esophagitis in patients who received fexuprazan 40 mg once daily was 99.1% at week 8, which was equal to the rate observed for patients receiving esomeprazole 40 mg once daily (99.1%).[1−3] Fexuprazan was well tolerated and much more effective than esomeprazole at treating heartburn and other general symptoms in patients with moderate to severe symptoms, and the relief effect lasted overnight.[1−3] Additionally, unlike PPIs, the metabolism of fexuprazan is independent of CYP2C19; thus, therapeutic applications can be achieved without the need to consider genetic polymorphism.[1,4]

Fexuprazan is commonly prepared from compound **1** (Figure 1) through sulfonamidation, reduction, oxidation, and reduced-amination reactions. Considering that methyl 5-(2,4-difluorophenyl)-4-methoxy-1*H*-pyrrole-3-carboxylate **1** is the key intermediate for the synthesis of fexuprazan, its synthesis is well worth studying. Currently, there are four reported synthesis routes of intermediate **1**, three of which are shown in Scheme 1.

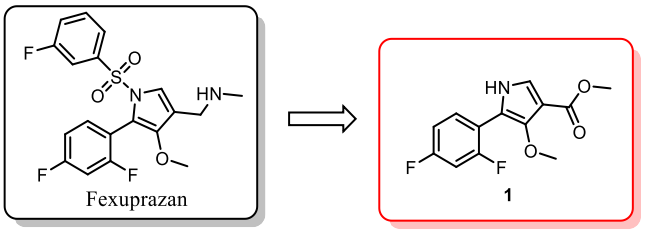

Figure 1. Fexuprazan and its key intermediate **1**.

The first route for the synthesis of intermediate **1** utilized 2-amino-2-(2,4-difluorophenyl)acetic acid **2** and dimethyl 2-(methoxymethylene)malonate **3** as the raw materials and involved nucleophilic substitution, cyclization reaction, and hydrolysis to obtain methyl 5-(2,4-difluorophenyl)-4-hydroxy-1*H*-pyrrole-3-carboxylate **6**; then, methylation with (diazomethyl)tri-methylsilane **7** afforded target intermediate **1** (Scheme 1A).[5] The total yield of intermediate **1** in this route

Received: May 12, 2024
Revised: July 17, 2024
Accepted: July 18, 2024
Published: August 23, 2024

Scheme 1. Synthesis Routes of the Key Intermediate 1

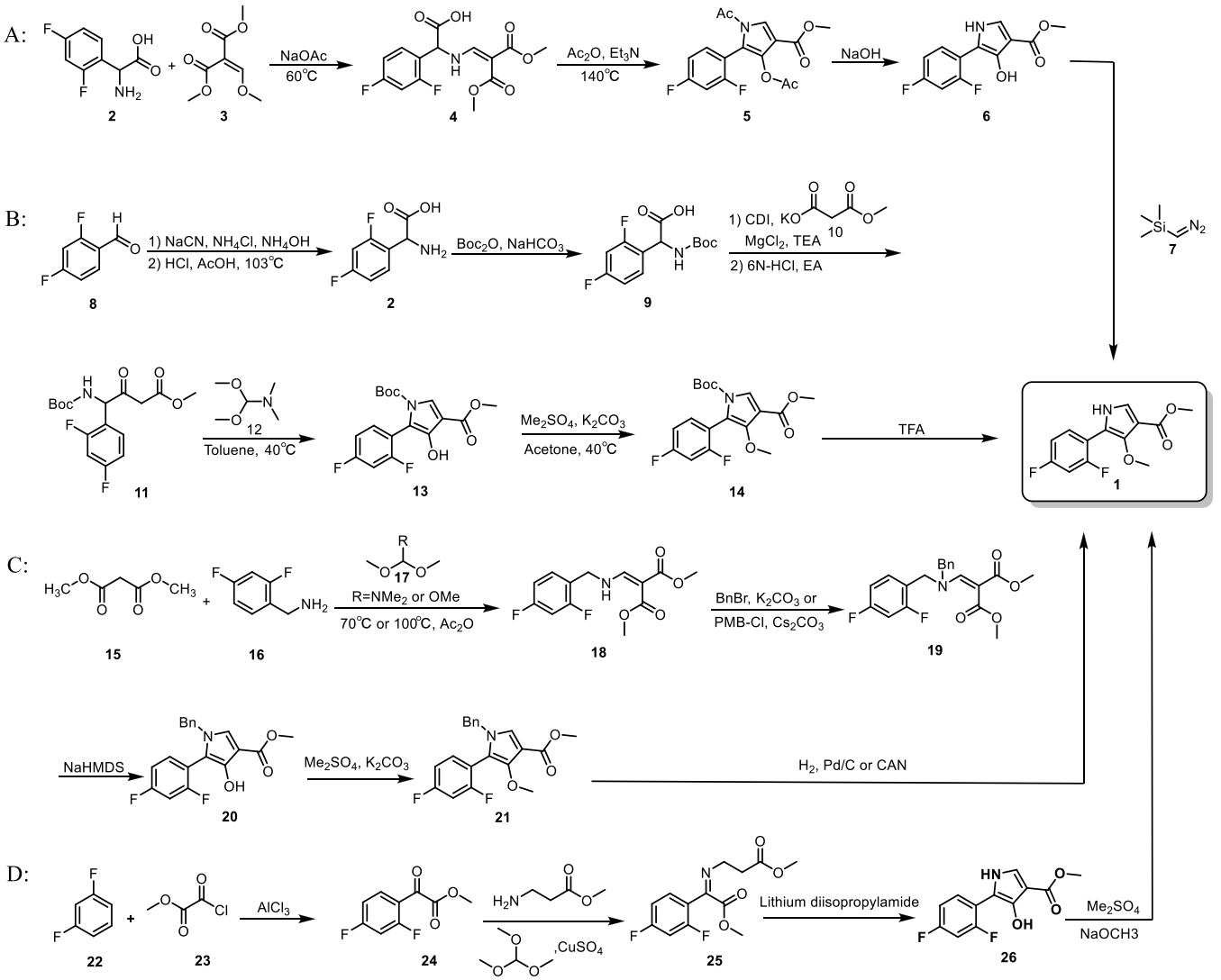

Scheme 2. Original Route and Optimized Route for the Synthesis of the Key Intermediate[a]

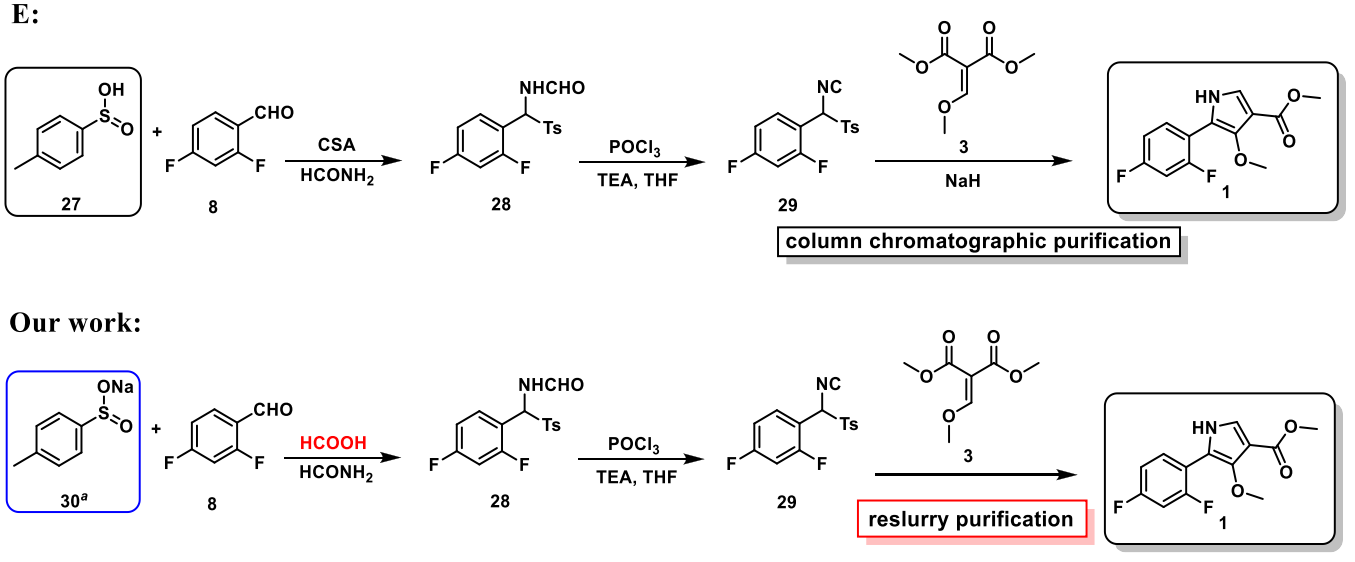

[a]**30**: stability: stable at room temperature and pressure, avoid contact with strong oxidizers. Slightly soluble in water. Storage conditions: keep the container sealed and store in a cool, dry place.

https://doi.org/10.1021/acsomega.4c04507
ACS Omega 2024, 9, 37942−37952

Scheme 3. Probable Mechanism of the Cyclization Reaction

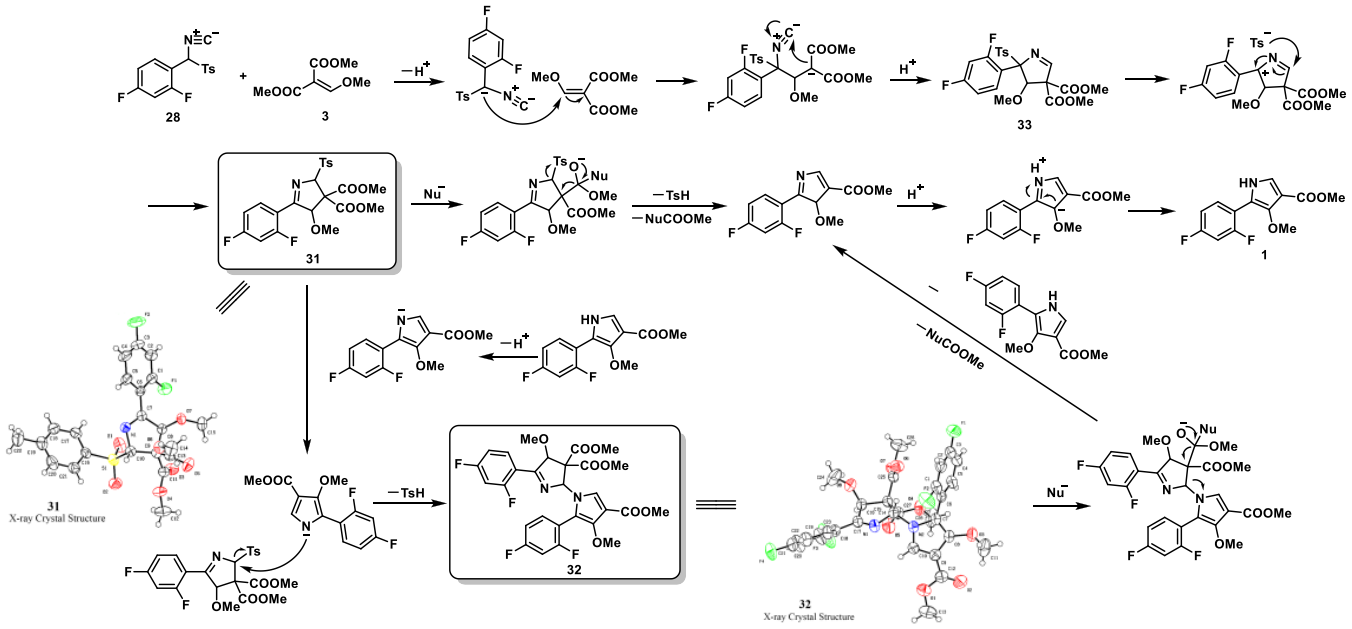

was only 9.0%, and the raw materials were expensive and scarce, making the procedure impractical on a large scale. Although the cheaper 2,4-difluorobenzaldehyde **8** was used in the second route (Scheme 1B) to improve the yield, it was not suitable for industrial production due to the lengthy reaction steps and usage of highly toxic reagents, such as sodium cyanide and dimethyl sulfate.[6] In the third method, (2,4-difluorophenyl)methanamine **16** and dimethyl malonate **15** were condensed to dimethyl 2-(((2,4-difluorobenzyl)amino) methylene) malonate **18** (Scheme 1C), followed by amino protection, cyclization reaction, methylation reaction, and finally deprotection to obtain intermediate **1**.[7] Although the method was inexpensive, the complicated purification processes and toxic dimethyl sulfate restricted its industrial production. In the fourth route, m-difluorobenzene reacted with methyl oxalyl chloride to yield compound **24**. After undergoing dehydration and intramolecular ring formation reactions, it led to compound **26**. Finally, it reacted with dimethyl sulfate to produce intermediate **1**.[8] The methods used to synthesize intermediate **1** involve several disadvantages, including the utilization of expensive raw materials and hazardous chemicals, lengthy reaction routes, and low overall yields.

Herein, we used the fifth method[9] (Scheme 2E) with a shorter route for optimization. The raw materials of the original route were expensive and commercially unavailable at bulk scale, and the purification method was complicated, resulting in a total yield of just 24.3%. The improved, three-step procedure (Scheme 2) for the synthesis of intermediate **1** by starting with commercially available sodium *p*-tolylsulfinate **30** was reported, which afforded target compound **1** with 99.8% purity and 68.1−69.6% overall yield. Notably, we proposed a mechanism for the last step (Scheme 3) in which the unreported compounds **31** and **32** were converted into key intermediate **1** by a one-pot reaction and purified by reslurry, resulting in a significantly improved yield.[10,11]

2. RESULTS AND DISCUSSION

A new method was adopted to synthesize key intermediate **1** of fexuprazan, sodium *p*-tolylsulfinate and 2,4-difluorobenzaldehyde as starting materials reacted with formamide under acidic conditions to obtain compound **28** with a 94.9% isolated yield. The isocyanide compound **29** was then obtained by dehydrating compound **28** with phosphorus oxychloride, with a yield of 84.8%. Finally, under strong base conditions, compound **29** reacted with dimethyl 2-(methoxymethylene) malonate **3** to yield key intermediate **1** in 85.8% yield. In contrast to other reported synthesis routes, the three-step workup method used to remove impurities comprised washing and reslurry rather than column chromatographic purification. This method produced a total yield of more than 68% and was notable for its novel approach, low cost, mild reaction conditions, and simple purification method.

2.1. Preparation of *N*-((2,4-Difluorophenyl)(tosyl)-methyl)formamide 28. Because 4-methylbenzenesulfinic acid is expensive, sodium *p*-tolylsulfinate was selected as the starting material. The sodium salt was converted to free acid by adding excess acid, and compound **28** was obtained by a one-pot method. The effects of various acids on the yield were investigated, including organic acid (formic acid), mineral acid (hydrochloric acid), and camphorsulfonic acid as catalysts, as reported in the original literature.[9] As shown in Table 1, the highest yield of only 67.3% was obtained using low-cost formic acid; therefore, the reaction conditions were further examined.

Table 1. Effect of Acid on the Synthesis of Compound 28[a]

entry	acid	time (h)	yield[c] (%)
1	hydrochloric acid[b]	10	46.5
2	formic acid	10	67.3
3	camphorsulfonic acid	10	47.9

[a]Reaction conditions: sodium *p*-tolylsulfinate (0.030 mol), 2,4-difluorobenzaldehyde (0.030 mol), formamide (0.300 mol), and acid (0.060 mol), 65 °C. [b]Hydrochloric acid with quality percent of 36.0−38.0%. [c]Yield of the isolated product.

https://doi.org/10.1021/acsomega.4c04507
ACS Omega 2024, 9, 37942−37952

The reaction parameters were optimized using the response surface method (RSM), a statistical and mathematical technique for process improvement.[12−14] The most commonly used experimental design method in RSM is Box−Behnken design (BBD), which involves fewer experiments than the central composite design and does not arrange all test factors into a high-level test combination at the same time, especially for certain tests with safety requirements or special needs.[15−19] In this experiment, BBD was used to construct the experimental design and analysis. There were three factors with three levels each (Table 2), and a total of 15 experiments,

Table 2. Codes and Levels of Factors for BBD[a]

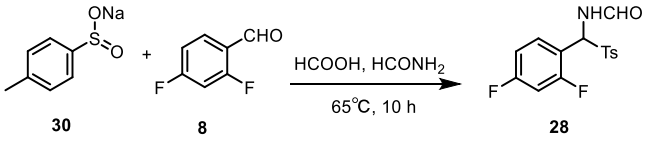

		actual levels of coded factors		
factors	coded	−1	0	1
2,4-difluorobenzaldehyde (eq)	A	1	1.5	2
formamide (eq)	B	5	10	15
formic acid (eq)	C	2	3.5	5

[a]Reaction conditions: sodium *p*-tolylsulfinate (5 g, 1.0 equiv). The time was determined based on observation during the reaction (after 10 h of reaction, a large amount of solid precipitated in the reaction mixture and stirring became difficult).

including three central point experiments, were needed to achieve the best process conditions (Table 3). As shown in

Table 3. Results of the Designed Experiments Based on Box−Behnken

				yield[a] (%)	
entry	A	B	C	actual value	predicted value
1	0	−1	1	88.08	87.53
2	0	0	0	91.58	90.37
3	0	1	−1	85.16	85.71
4	0	0	0	90.37	90.37
5	−1	0	1	71.42	71.83
6	1	0	−1	88.73	88.32
7	−1	0	−1	66.60	66.44
8	−1	−1	0	69.23	69.38
9	1	1	0	92.89	92.75
10	1	−1	0	89.12	89.52
11	0	1	1	88.40	88.39
12	1	0	1	91.47	91.63
13	0	−1	−1	81.50	81.51
14	−1	1	0	71.60	71.21
15	0	0	0	89.17	90.37

[a]Isolated yield of **28**. The properties of the products obtained in 15 experiments are shown in Figure S4.

Table 3, these 15 experimental schemes were designed by Design-Expert 10 software, and the results were obtained through the actual experiment, from which the model was established to obtain the predicted value.

The precision, coefficient of determination R^2, coefficient of variation (CV), and residual analysis showed that the quadratic polynomial regression model we created was accurate. From Table 4, it could be inferred that the model accounted for 99.64% of the total variation, and the difference between the

Table 4. ANOVA on the Response Surface Quadratic Model about Yield

source	sum of squares	df	mean square	*F*-value	*P*-value prob > *F*
model	1179.00	9	131.00	154.09	0.0001[a]
A−A	868.61	1	868.61	1021.72	0.0001
B−B	12.80	1	12.80	15.06	0.0116
C−C	37.76	1	37.76	44.41	0.0011
AB	0.49	1	0.49	0.58	0.4820
AC	1.08	1	1.08	1.27	0.3105
BC	2.79	1	2.79	3.28	0.1299
A^2	233.17	1	233.17	274.27	0.0001
B^2	10.88	1	10.88	12.80	0.0159
C^2	30.45	1	30.45	35.82	0.0019
residual	4.25	5	0.85		
lack of fit	1.35	3	0.45	0.31	0.8217[b]
pure error	2.90	2	1.45		
cor total	1183.25	14			
std. dev. 0.92			pred *R*-square 0.9763		
R-squared 0.9964			CV% 1.10		
adj *R*-squared 0.9899			adeq precision 34.938		

[a]Significant. [b]Not significant.

value of R^2 (0.9964) and R_{Adj}^2 (0.9899) is significantly less than 0.2. The prediction coefficient R^2 of 0.9964 is preferably close to 1, indicating a strong correlation between the experimental results and the quadratic model. The *P* value and *F* value are the criteria used for testing the model's significance; the higher the *F* value, the lower the *P* value, suggesting the greater the model's significance.[20] The *F* value and *P* value for the model were 154.09 and 0.0001, respectively, as shown in Table 4. There was only a 0.01% probability that noise would result in a very large *F* value. In this analysis, the model was deemed significant if the *P* value was less than 5%, and very significant if the *P* value was less than 1%,[21] indicating that the model we established was highly significant. In this case, *A*, *B*, *C*, A^2, B^2, and C^2 were significant model terms, while AB, AC, and BC were insignificant ($P > 0.05$). Precision is determined by the signal-to-noise ratio, which should be greater than 4. The signal-to-noise ratio (34.938) indicated that this model could be used to explore the system design. The CV, which is frequently employed to express the accuracy and reproducibility of an assay, reflects the proportion of the entire experimental error as a percentage of the total mean.[17,22] The CV% score (1.10%) < 10% in this instance demonstrated that the model exhibited a high level of accuracy and reproducibility.[23] Figure 2A shows that the actual and predicted values were highly linear, with almost all points distributed along a straight line and no outliers.[24] Externally studentized residuals are used to search for outliers or significant values using a normal probability plot of the studentized residuals to test for residual normality. The residual distribution between 2 and −2 clearly matched the normal distribution, as shown in Figure 2B. As a result, this model is reliable and standard and can be used to assess the effectiveness of an experiment.

A 3D surface diagram illustrating the impact of the interaction of the two factors on the product yield was built to better study the interaction of the three variables. Figure 3

https://doi.org/10.1021/acsomega.4c04507
ACS Omega 2024, 9, 37942−37952

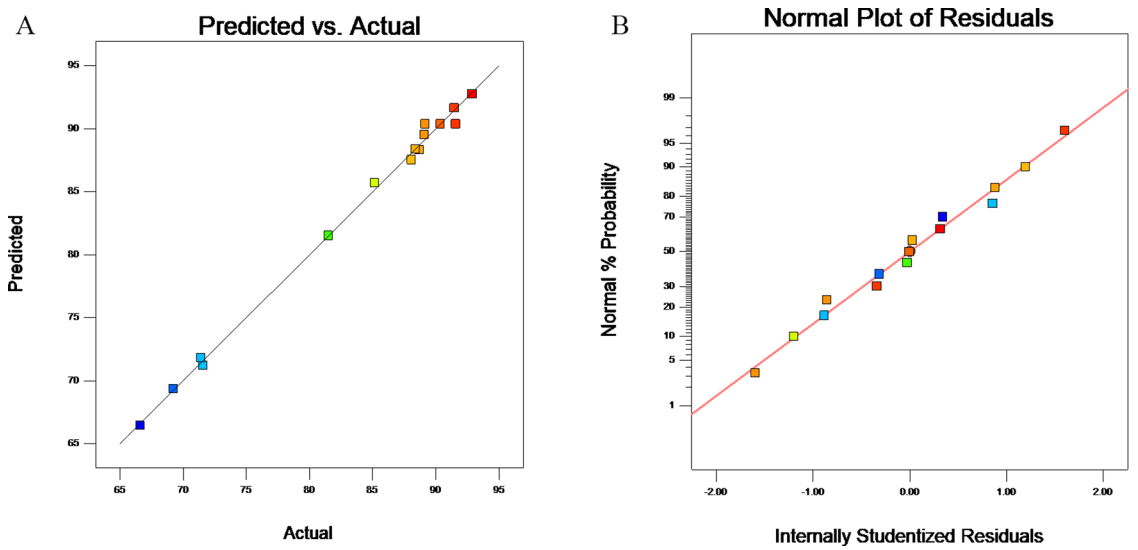

Figure 2. Diagnostic plots of the quadratic model of yield: (A) predicted against actual, (B) normal % probability against externally studentized residuals.

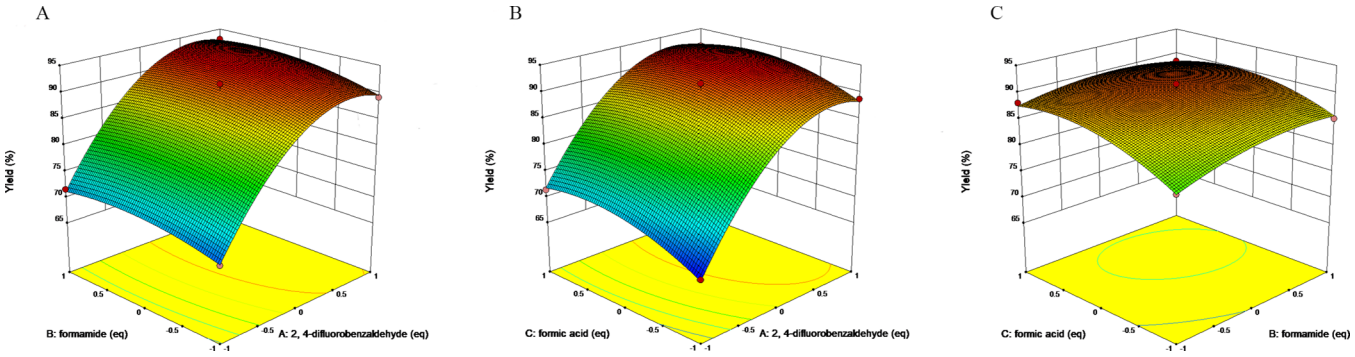

Figure 3. 3D surface plots of effects of binary interactions among factors on response value yield of compound **28**: (A) formamide and 2,4-difluorobenzaldehyde; (B) formic acid and 2,4-difluorobenzaldehyde; (C) formic acid and formamide.

displays the 3D response surface plots of a quadratic model in which two variables varied along the experimental range and one variable remained at the central level. Additionally, the degree of interaction between the two parameters varies, and the nonlinear relationship between the two affects the value of the product performance response.[25] The interaction between the two factors can be more easily interpreted from the interaction diagram in Figure 4. The degree of overlap of the two curves increases as the degree of the factor interactions decreases.[17] Figure 4A illustrates that under the same feed ratio of formic acid, the red curve represents the yield at B = 15, and the black curve represents the yield at B = 5. The red curve was higher than the black curve; thus, with increasing doses of A and B, the yield of compound **28** was higher. With an increase in A, the two curves gradually separated, which also indicated that A and B had obvious interactions. Similarly, Figure 4B,C shows that there was a clear interaction between A and C or B and C.

Through the aforementioned analysis, the three variables' values can be appropriately increased to obtain the ideal yield value. The ideal values of the input factors were determined using Design-Expert 10 software for numerical optimization as A = 1.83, B = 11.84, and C = 3.90, and the highest yield value was expected to be 94.3%. The optimal point predicted by the model was then used for three sets of simultaneous verification trials, and the average yield was 94.2% with an error of 0.1%, which was consistent with the value predicted, confirming the accuracy of the model. The total cost of route D in the first step is 6.7 times higher than that of our optimized method (Tables S4 and S6). The model was constructed using 2,4-difluorobenzaldehyde as unit 1, and the corresponding data can be found in the Supporting Information. Table S5 reveals that the cost of producing 1 kg of the product is comparable to the cost of using sodium *p*-tolylsulfinate as unit 1. Therefore, considering the actual raw material price at the time of production, we can opt for a more cost-effective method. The one-pot method is employed to streamline the synthesis process and simplify postprocessing. Finally, using the optimal conditions, we scaled up the reaction to 500 g and produced 884 g of compound **28** as a white solid with a purity of 97.1% in a 96.8% isolated yield.

2.2. Preparation of 2,4-Difluoro-1-(isocyano(tosyl)-methyl)benzene 29. Compound **29** was synthesized through the dehydration of compound **28** using phosphorus oxychloride under alkaline conditions. Initially, phosphorus oxychloride and compound **28** were combined, followed by the gradual addition of triethylamine to the reaction mixture.[26] To achieve the maximum reaction yield, we investigated several factors including the reaction solvent, the feed ratio of phosphorus oxychloride, and the reaction temperature. We

https://doi.org/10.1021/acsomega.4c04507
ACS Omega 2024, 9, 37942−37952

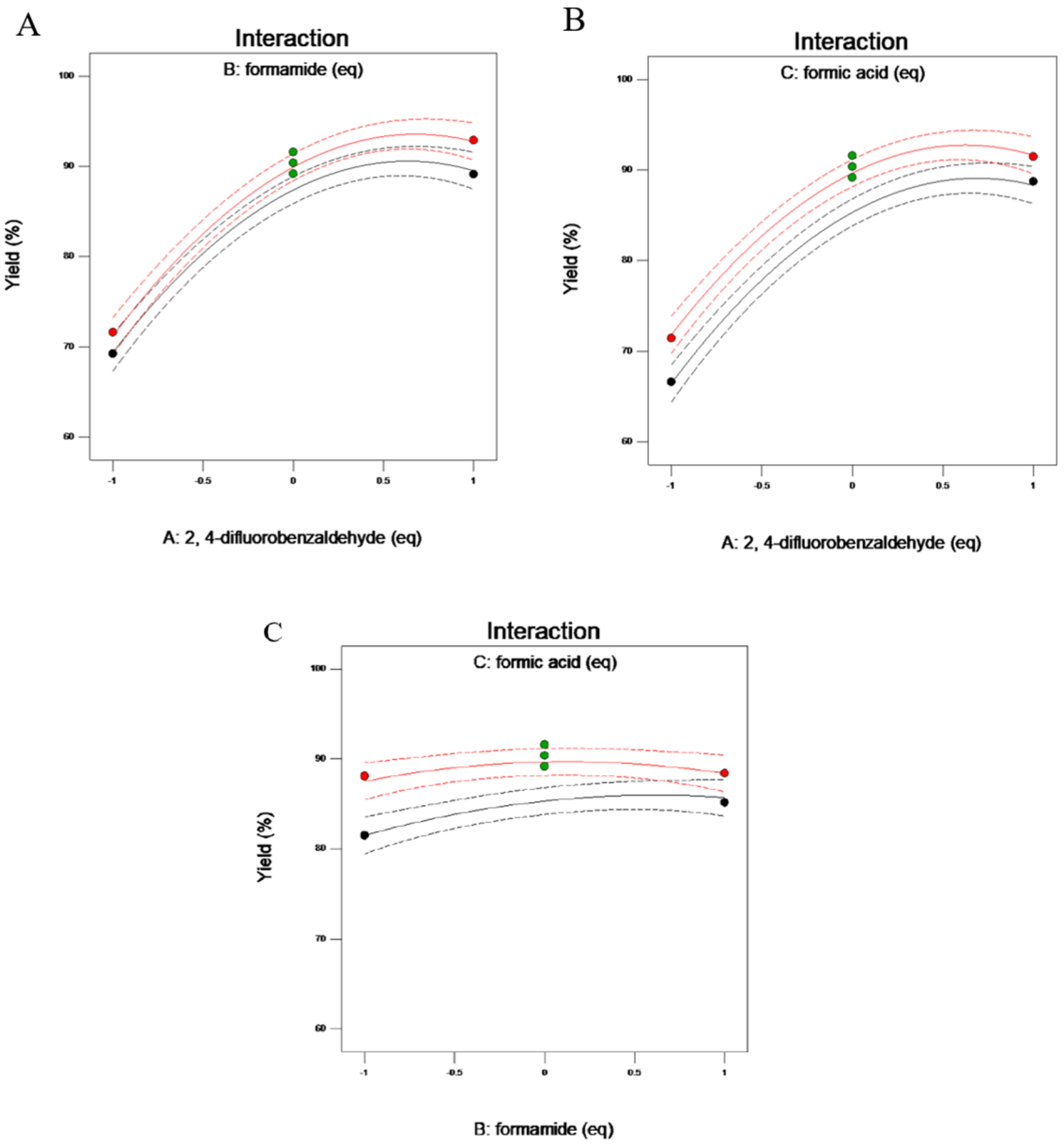

Figure 4. Interaction plot between different factors: (A) interaction plot of formamide and 2,4-difluorobenzaldehyde, under the same formic acid, the red curve represents the yield at the B = 15 and the black curve represents the yield at B = 5; (B) interaction plot of formic acid and 2,4-difluorobenzaldehyde, under the same formamide, the red curve represents the yield at the C = 5 and the black curve represents the yield at C = 2; (C) interaction plot of formic acid and formamide, under the same 2,4-difluorobenzaldehyde, the red curve represents the yield at the A = 2 and the black curve represents the yield at A = 1.

examined the impact of the reaction solvent on the yield by comparing entries 1−3 in Table 5. The results indicated that using THF as the solvent resulted in a higher yield compared to DCM and CH_3CN. Among the different quantities of $POCl_3$ tested (entries 3−6 in Table 5), 3.5 equiv yielded the highest result. Analyzing entries 5 and 5, 7−9 in Table 5, we observed that as the reaction temperature increased beyond 0 °C, the yield decreased due to the presence of more impurities with all variables being the same. Further investigation revealed that the optimal reaction temperature was 0 °C. Finally, employing the aforementioned reaction conditions, we obtained compound **29** with a purity of 99.4% and a yield of 84.7% on a 500 g scale.

2.3. Preparation of Methyl 5-(2,4-Difluorophenyl)-4-methoxy-1*H*-pyrrole-3-carboxylate 1. According to published research, compound **29** underwent a reaction with dimethyl 2-(methoxymethylene) malonate **3** in the presence of sodium hydride to obtain key intermediate **1**.[9] However, the procedure described in the literature yielded poor results, requiring purification through silica gel column chromatography.[9] Therefore, the conditions of the cyclization reaction were thoroughly investigated, as presented in Table 6. HPLC analysis of the reaction solution revealed the presence of two impurities in the acetonitrile solvent, with respective contents of 25.12 and 21.30%. The Supporting Information identified these impurities as compound **31** and compound **32**. The reaction temperature and time significantly influenced the chemical reaction rate and had varying effects on the yield. Therefore, we investigated the reaction temperature and time, as shown in entries 4−9 of Table 6. Increasing the temperature

https://doi.org/10.1021/acsomega.4c04507
ACS Omega 2024, 9, 37942−37952

Table 5. Optimization for Synthesizing Compound 29[a]

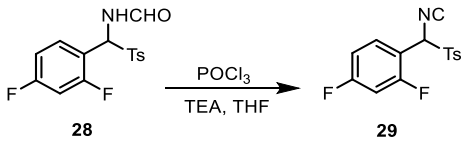

28 29

entry	solvent	$POCl_3$ (equiv)	T (°C)	HPLC[b] (%)
1	CH_2Cl_2	2.0	0	trace[c]
2	CH_3CN	2.0	0	trace[c]
3	THF	2.0	0	70.52
4	THF	3.0	0	86.40
5	THF	3.5	0	92.36
6	THF	4.0	0	86.87
7	THF	3.5	−10	63.51
8	THF	3.5	10	71.82
9	THF	3.5	25	16.88
10[d]	THF	3.5	0	99.43[e]

[a]Reagents and conditions: **28** (5 g, 1.0 equiv), $POCl_3$, TEA (6.0 equiv), THF (60 mL). [b]Numbers listed indicate conversion which were assessed by HPLC analysis. [c]By TLC analysis, the product was oil-like, no solids were precipitated. [d]**28** (500 g). [e]Purity of **29** after reslurry.

and time gradually decreased the content of compound **1** while increasing the content of compound **32**, indicating that a higher reaction temperature or longer reaction time converted compound **1** into compound **32**. It is important to note that the total content of these three compounds (**1**, **31**, and **32**) ranged from 86.99 to 90.74%, making them the main components in the reaction solution. Furthermore, we examined the effect of NaH dosage on the reaction, which revealed that increasing the NaH dosage significantly increased the content of compound **1**. When NaH was used in 8 equiv, the content of **1** reached its maximum value (88.29%). However, further increasing the NaH dosage resulted in a decrease in the content of **1** and the generation of new impurities (Table 6, entries 9−14). Although a higher yield was achieved with 8 equiv of NaH, it also led to the production of a large amount of H_2, posing safety hazards and making it unsuitable for mass production.

Through the analysis of experimental data, we proposed a plausible reaction mechanism, as illustrated in Scheme 3. Initially, deprotonation of compound **29** using NaH generated a carbanion, which subsequently attacked the double bond of compound **3**, leading to the cyclization and formation of compound **33**. The tosyl (Ts) group attached to compound **33** underwent rearrangement through a 1,3 shift, resulting in the formation of impurity **31**. The nucleophilic attack on impurity **31** caused the expulsion of the tosyl group, yielding compound **1**. Compound **1**, upon deprotonation by the base reagent, underwent exchange with the tosyl group on impurity **31**, generating impurity **32**. Finally, impurity **32** was attacked by a nucleophilic reagent, leading to the formation of the desired 2-molecule **1**. Ultimately, both impurities **31** and **32** were converted into the target product **1**. Based on this mechanism, we hypothesize that an excess amount of the base reagent (greater than 2.0 equiv) is required to facilitate deprotonation of the hydrogen on the carbon and subsequently act as a nucleophilic reagent. When using only 1.1 equiv of NaH, only the first step of deprotonation is completed, resulting in the main components in the reaction solution being compound **1**, **31**, and **32**. However, employing 2.0 equiv of sodium hydride leads to a content of compound **1** of only 66.10%. This discrepancy may be attributed to the relatively poor nucleophilicity of NaH. Under conditions of excess NaH,

Table 6. Optimization for Synthesizing Key Intermediate 1[a]

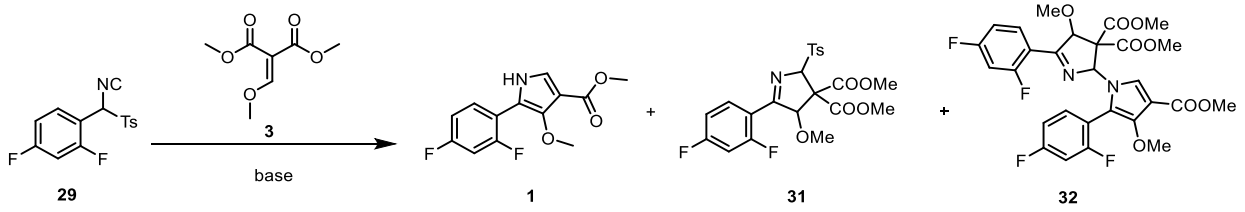

29 1 31 32

entry	base (equiv)	solvent	T (°C)	time (h)	HPLC[b] (%) 1	31	32
1	NaH (1.1)	CH_3CN	r.t.	1	43.84	25.12	21.30
2	NaH (1.1)	DMF[c]	r.t.	1	24.35	21.62	1.49
3	NaH (1.1)	THF	r.t.	1	39.72	18.61	7.31
4	NaH (1.1)	CH_3CN	−10	1	45.79	22.71	18.49
5	NaH (1.1)	CH_3CN	40	1	39.94	23.47	27.33
6	NaH (1.1)	CH_3CN	70	1	35.49	22.50	29.42
7	NaH (1.1)	CH_3CN	r.t.	0.5	46.24	23.33	20.01
8	NaH (1.1)	CH_3CN	r.t.	3	43.07	21.96	25.39
9	NaH (1.1)	CH_3CN	r.t.	10	41.73	21.27	25.46
10	NaH (2.0)	CH_3CN	r.t.	1	66.10	13.56	11.87
11	NaH (4.0)	CH_3CN	r.t.	1	72.82	7.28	7.50
12	NaH (6.0)	CH_3CN	r.t.	1	85.43	ND[d]	1.61
13	NaH (8.0)	CH_3CN	r.t.	1	88.29	ND[d]	0.55
14	NaH (10)	CH_3CN	r.t.	1	86.48	ND[d]	ND[d]
15	NaH (15)	CH_3CN	r.t.	1	75.75	0.34	0.30

[a]Reagents and conditions: **29** (0.5 g), **3** (1.0 equiv), solvent (15 mL). [b]Numbers listed indicate conversion which were assessed by high-performance liquid chromatography (HPLC) analysis of the organic layer. [c]Explosion hazards of sodium hydride in DMF. [d]Not detected.

https://doi.org/10.1021/acsomega.4c04507
ACS Omega 2024, 9, 37942−37952

Table 7. Optimization of the Reaction Conditions[a]

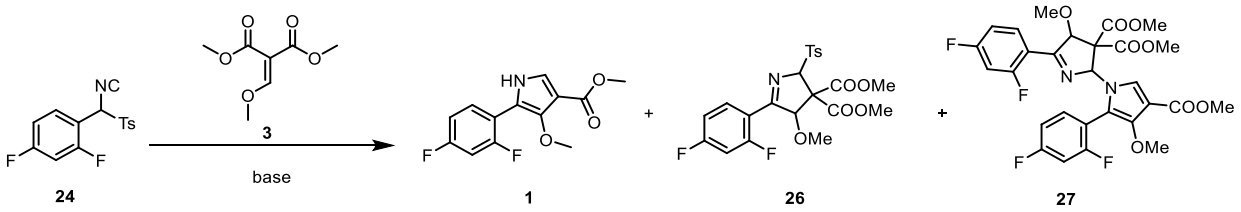

				HPLC[b] (%)		
entry	base (equiv)	T[c] (°C)	time (h)	**1**	**31**	**32**
1	DBU (3.0)	r.t.	1	48.00	29.79	ND[d]
2	DBU (3.0)	r.t.	10	37.55	38.21	1.31
3	Na_2CO_3(3.0)	60	10	NR[e]	NR[e]	NR[e]
4	K_2CO_3(3.0)	60	10	NR[e]	NR[e]	NR[e]
5	Cs_2CO_3(3.0)	r.t.	1	3.39	28.65	ND[d]
6	Cs_2CO_3(3.0)	80	10	20.13	10.38	18.03
7	K_3PO_4(3.0)	r.t.	1	11.17	11.10	ND[d]
8	K_3PO_4(3.0)	60	10	33.29	36.67	ND[d]
9	$NaOCH_3$(1.2)	r.t.	1	19.21	10.77	ND[d]
10	$NaOCH_3$(3.0)	r.t.	1	72.93	19.19	1.06
11	$NaOCH_3$(3.0)	r.t.	6	76.22	16.96	1.01
12	*t*-BuOK(1.2)	r.t.	1	33.27	11.60	7.59
13	*t*-BuOK(3.0)	r.t.	1	38.72	0.19	ND[d]
14	*t*-BuOK(3.0)	r.t.	6	36.20	0.23	ND[d]
15	NaOH (1.2)	r.t.	1	57.87	24.38	10.09
16	NaOH (3.0)	r.t.	1	93.74	0.40	1.55
17	NaOH (3.0)	r.t.	3	92.53	ND[d]	1.19

[a]Reagents and conditions: **29** (0.5 g), **3** (1.0 equiv), solvent: CH_3CN (15 mL). [b]Numbers listed indicate conversion which were assessed by HPLC analysis of the organic layer. [c]r.t. = 20−25 °C. [d]Not detected. [e]No reaction.

acetonitrile undergoes deprotonation to form $-CH_2CN$, which acts as a nucleophilic reagent and converts impurities **31** and **32** into compound **1**, thereby significantly improving the reaction yield.

To test this hypothesis, we synthesized compounds **31** and **32** and subjected them to reactions with commonly employed and potent nucleophilic alkaline reagents, namely, sodium hydroxide and sodium methoxide. We were delighted to witness the transformation of both **31** and **32** into compound **1**. Given that NaH is unsuitable for industrial-scale production, we explored alternative bases, particularly focusing on commonly used inorganic bases that facilitate subsequent treatments. The details of our investigations are presented in Table 7.[27−29] From entries 1−8, it was evident that increasing the reaction temperature or duration did not significantly enhance the reaction yield when using DBU, Na_2CO_3, K_2CO_3, Cs_2CO_3, or K_3PO_4 as alkaline reagents. However, when the stronger alkaline reagent $NaOCH_3$ was employed (Table 7, entries 9−11), the content of compound **1** in the reaction solution noticeably increased, while 17.0% of impurity **31** was not converted. Conversely, the use of the even stronger alkaline reagent *t*-BuOK (Table 7, entries 12−14) led to the generation of new impurities, resulting in a significant decline in the yield of compound **1**. Consequently, sodium hydroxide (NaOH) was selected as the alkaline reagent due to its strong alkalinity and affinity. Entries 15−17 demonstrated a significant conversion of impurities **31** and **32** into desired compound **1**, leading to a considerable improvement in the reaction yield.

Subsequently, with NaOH as the alkaline reagent, we explored the reaction solvent and the NaOH feeding ratio, as presented in Table 8. Ultimately, the highest yield was achieved by employing 2.5 times the amount of NaOH as the alkaline reagent and using acetonitrile as the reaction solvent at room temperature for 1 h.

Table 8. Optimization of the Reaction Conditions with Sodium Hydroxide as Base[a]

			HPLC[b] (%)		
entry	base (equiv)	solvent	**1**	**31**	**32**
1	NaOH (3.0)	C_2H_5OH	3.72	0.30	10.09
2	NaOH (3.0)	CH_2Cl_2	46.44	22.52	ND[c]
3	NaOH (3.0)	THF	88.23	0.30	4.07
4	NaOH (3.0)	acetone	92.01	1.51	1.64
5	NaOH (2.0)	CH_3CN	89.19	4.60	2.06
6	NaOH (2.5)	CH_3CN	93.11	0.47	1.54

[a]Reagents and conditions: **29** (0.5 g), **3** (1.0 equiv), solvent: CH_3CN (15 mL), r.t. = 20−25 °C, 1 h. [b]Numbers listed indicate conversion which were assessed by HPLC analysis of the organic layer. [c]Not detected.

Then, the investigation focused on the solvents used for the slurry of the crude product, as shown in Table 9. Compound **1** purity was below 99% when the ethyl acetate/*n*-heptane ratio

Table 9. Screening of Solvent during Post-Treatment of 1

entry	solvent (ratio)	purity (%)	yield (%)
1	ethyl acetate/*n*-heptane (2:15)	95.13	88.2
2	ethyl acetate/*n*-heptane (3:15)	99.24	85.8
3	ethyl acetate/*n*-heptane (4:15)	99.73	84.6
4	ethyl acetate/*n*-heptane (3:17)	99.17	86.3
5	ethyl acetate/*n*-heptane (3:20)	98.34	87.5

https://doi.org/10.1021/acsomega.4c04507
ACS Omega 2024, 9, 37942−37952

was 3:20 or less. At a 4:15 ethyl acetate/*n*-heptane ratio, the purity reached 99.73%; however, the yield was also reduced. Consequently, reslurrying with ethyl acetate and *n*-heptane (3:15) yielded a white solid. Ultimately, key intermediate **1** was obtained with a purity of 99.2% and a yield of 85.8% on a 400 g scale.

2.4. Quality Detection and Yield Stability of Intermediate 1. The new technique was carried out for sodium *p*-tolylsulfinate **30** on a 100 g scale with the optimization condition in hand to confirm the robustness and scalability of this procedure, as indicated in Table 10. The technique has

Table 10. Results of Three Batches of Experiment[a]

entry	mass of **30**	loss on drying	residue on ignition	water	total yield	purity
1	100 g	0.08%	0.04%	0.24%	69.6%	99.59%
2	100 g	0.04%	0.02%	0.20%	68.5%	99.13%
3	100 g	0.06%	0.01%	0.21%	68.1%	99.47%

[a]Product was dissolved in ethyl acetate and then filtered to remove insoluble impurities.

good yield stability and potential for industrial application, as evidenced by the overall yield of 68.1−69.6%, purity of more than 99%, loss on drying of less than 1.0%, and residue on ignition of less than 0.5%.

3. CONCLUSIONS

In conclusion, we have developed a synthetic approach to synthesize the key intermediate of fexuprazan (**1**) from sodium *p*-tolylsulfinate with a much lower cost and higher yield than those of previous approaches. The three-step reaction produced the key intermediate **1**, the overall yield was greater than 68% and the purity was greater than 99%. The process parameters of the first step were optimized using the Box−Behnken experimental design, and impurities **31** and **32** were converted into the desired product **1** by studying the reaction mechanism. The current process was successfully tested on a 500 g scale using a simple purification method, providing a new synthetic strategy for the synthesis of the key fexuprazan intermediate.

4. EXPERIMENTAL SECTION

4.1. Materials and Methods. Unless otherwise specified, commercially obtained solvents and reagents were used in the experiments without further purification. Analytical thin-layer chromatography (TLC) was used to monitor the reactions, which were then visualized under ultraviolet light (254 and 365 nm). HPLC analysis on a JASCO pu-1580 system with a JASCO UV-1575 detector was used to determine the chemical purity. Using isocratic elution of water and methanol/acetonitrile at a flow rate of 1.0 mL/min, the analytes were separated using a ZORBAX Eclipse XDB-C18 (4.6 × 250 mm^2, 5 μm particle size) column. HPLC analysis on a Waters Alliance 2695 system with W2489 ChA 254 nm detector was used to determine quality detection (chemical purity). Using gradient elution of Mobile phase A (dipotassium hydrogen phosphate 1.74 g into 1000 mL water, then add trifluoroacetic acid and mix well, then adjust to pH 2.80−2.90) and Mobile phase B (methanol:acetonitrile = 45:55 (v/v)) at a flow rate of 1.0 mL/min, the analytes were separated using a Kromasil C8 (4.6 mm × 250 mm, 5 μm) column. Using DMSO-d6 as the test solvent and TMS as an internal reference, NMR spectra were captured using a Bruker Avance 600/400 MHz spectrometer. High-resolution mass spectrometry (HRMS) data were produced by using an Agilent Q-TOF 6530/6550 mass spectrometer. Design-Expert 10 software was used to create these experimental schemes in the first step. The differential scanning calorimetry (DSC) curves and thermogravimetric analysis (TGA) were investigated with Netzsch differential scanning calorimeter (DSC 214) at the heating rate of 5 °C/min in the range of room temperature to 500 °C in a nitrogen atmosphere. Sealed gold-plated high-pressure DSC crucibles were used for the evaluation.

4.2. Synthesis of *N*-((2,4-Difluorophenyl)(tosyl)-methyl)formamide 28. Sodium *p*-tolylsulfinate **30** (500 g, 2.81 mol), 2,4-difluorobenzaldehyde **8** (730 g, 5.14 mol), formic acid (504 g, 10.9 mol), and formamide (1496 g, 33.2 mol) were added to a 5 L flask, and the mixture was mechanically stirred for 10 h at 65 °C. After cooling to room temperature, water (2.5 L) was added, and the mixture was mechanically stirred for 0.5 h, and a white crude product was obtained by filtration under reduced pressure. The white crude product was filtered and washed with hexane (2 L × 3) and water (2 L × 3) dried in a blast drying oven at 60 °C for 48 h to give 884 g. (96.8% yield.) HPLC purity: 97.1%. ^{1}H NMR (600 MHz, DMSO-d_6) δ 9.93 (dd, J = 10.3, 1.5 Hz, 1H), 8.03 (d, J = 1.3 Hz, 1H), 7.74 (td, J = 8.5, 8.4, 6.3 Hz, 1H), 7.69−7.65 (m, 2H), 7.46 (d, J = 8.0 Hz, 2H), 7.35 (td, J = 9.7, 9.7, 2.6 Hz, 1H), 7.28 (td, J = 8.6, 8.5, 2.6 Hz, 1H), 6.52 (d, J = 10.4 Hz, 1H), 2.41 (s, 3H). ^{13}C NMR (151 MHz, DMSO-d_6) δ163.1 (dd, J = 249.8, 12.6 Hz), 160.6, 160.4 (dd, J = 250.7, 12.7 Hz), 145.4, 132.8, 131.7 (dd, J = 10.4, 3.6 Hz), 130.0, 129.1, 114.6 (dd, J = 14.3, 3.8 Hz), 112.3 (dd, J = 21.8, 3.4 Hz), 104.2 (t, J = 26.3, 26.3 Hz), 63.3 (d, J = 2.4 Hz), 21.2. HRMS (ESI-TOF) m/z: $[M + Na]^+$ calcd for $C_{15}H_{13}NO_3NaSF_2$, 348.0482; found, 348.0481.

4.3. Synthesis of 2,4-Difluoro-1-(isocyano(tosyl)-methyl)benzene 29. Tetrahydrofuran (3.5 L) and **28** (500 g, 1.54 mol) were placed in a 10 L three-necked flask equipped with an overhead stirrer, an addition funnel, and a temperature probe. The solution was stirred at 25 °C after adding 825 g (5.38 mol) of phosphorus oxychloride. Triethylamine (933 g, 9.22 mol) was added gradually after the solution had been cooled to 0 °C while keeping the internal reaction temperature 0 °C. Following the completion of the triethylamine addition, the reaction continued for 30 min. The reaction was quenched by slowly adding the reaction solution to aqueous solution of NaOH (10 L, 2 mol/L), then ethyl acetate (10 L) was added and the mixture was mechanically stirred for 0.5 h. After concentrating the organic layer, it was reslurry with *n*-propanol (0.3 L) to give a yellow solid. The yellow solid was filtered and the filter cake is rinsed with *n*-propanol (0.1 L × 2) to produce a yellowish solid dried in a blast drying oven at 40 °C (400 g, 84.7% yield). HPLC purity: 99.4%. ^{1}H NMR (600 MHz, DMSO-d_6) δ 7.73−7.69 (m, 2H), 7.56−7.52 (m, 2H), 7.45−7.40 (m, 2H), 7.26 (td, J = 8.6, 8.3, 2.2 Hz, 1H), 7.10 (s, 1H), 2.46 (s, 3H). ^{13}C NMR (151 MHz, DMSO-d_6) δ 164.3, 163.8 (dd, J = 251.2, 12.2 Hz), 160.4 (dd, J = 255.0, 13.0 Hz), 146.8, 131.5 (dd, J = 10.9, 3.2 Hz), 130.3, 130.2, 129.9, 112.6 (dd, J = 22.2, 3.4 Hz), 111.3 (dd, J = 13.0, 3.8 Hz), 104.9 (t, J = 25.9, 25.9 Hz), 69.4, 21.3. HRMS (ESI-TOF) m/z: $[M + Na]^+$ calcd for $C_{15}H_{11}NO_2F_2NaS$, 330.0376; found, 330.0369.

4.4. Synthesis of Dimethyl 5-(2,4-Difluorophenyl)-4-methoxy-2-tosyl-2,4-dihydro-3*H*-pyrrole-3,3-dicarboxylate 31 and Trimethyl 5,5′-Bis(2,4-difluorophenyl)-4,4′-

https://doi.org/10.1021/acsomega.4c04507
ACS Omega 2024, 9, 37942−37952

dimethoxy-2′,4′-dihydro-3′*H*-[1,2′-bipyrrole]-3,3′,3′-tricarboxylate 32. Compound **29** (10.0 g, 0.03 mol) and dimethyl methoxymethylenemalonate **3** (5.7 g, 0.03 mol) were added to the reaction flask and dissolved with acetonitrile (90 mL). Sodium hydride (0.86 g, 0.04 mol) was added in batches and stirred at room temperature for 1 h. After the reaction was complete, water (200 mL) and ethyl acetate (200 mL) were added for extraction to concentrate the collected organic layer. Then, **31**, **32** were isolated by silica gel column chromatography and obtained as one white solid (**31**, 2.1 g, 13.2% yield) and another white solid (**32**, 0.9 g, 4.7% yield).

31: HPLC purity: 99.7%. ^{1}H NMR (600 MHz, DMSO-d_6) δ 7.72 (td, J = 8.6, 8.5, 6.5 Hz, 1H), 7.70−7.66 (m, 2H), 7.49−7.43 (m, 1H), 7.42 (d, J = 8.2 Hz, 2H), 7.20 (td, J = 8.4, 8.4, 2.5 Hz, 1H), 6.11 (d, J = 1.2 Hz, 1H), 5.79−5.64 (m, 1H), 3.80 (s, 3H), 3.70 (s, 3H), 3.43 (s, 3H), 2.40 (s, 3H). ^{13}C NMR (151 MHz, DMSO-d_6) δ 174.0 (d, J = 2.5 Hz), 164.6 (dd, J = 252.9, 12.6 Hz), 161.1 (dd, J = 255.8, 13.0 Hz), 145.3, 134.7, 132.3 (dd, J = 10.6, 4.3 Hz), 129.6, 129.2, 116.4 (dd, J = 12.3, 3.5 Hz), 112.7 (dd, J = 22.0, 3.2 Hz), 105.0 (t, J = 26.2, 26.2 Hz), 91.1, 89.9 (d, J = 3.3 Hz), 66.3, 59.8, 53.3, 53.2, 21.1. HRMS (ESI-TOF) m/z: [M + Na]$^+$ calcd for $C_{22}H_{21}NO_7F_2NaS$, 504.0904; found, 504.0901.

32: HPLC purity: 99.7%. 1H NMR (600 MHz, DMSO-d6) δ 8.01 (q, J = 8.0, 8.0, 7.9 Hz, 1H), 7.46 (ddd, J = 18.3, 9.2, 4.6 Hz, 3H), 7.25 (td, J = 8.4, 8.3, 2.5 Hz, 2H), 7.08 (s, 1H), 6.61 (d, J = 102.1 Hz, 1H), 5.87 (d, J = 60.4 Hz, 1H), 3.70 (s, 3H), 3.62 (s, 3H), 3.58 (s, 3H), 3.45 (s, 3H), 3.39 (s, 3H). 13C NMR (151 MHz, DMSO-d6) δ 170.9, 166.8, 166.1, 165.5 (d, J = 12.5 Hz), 163.8 (d, J = 12.7 Hz), 162.5, 162.2 (d, J = 48.7 Hz), 160.7 (d, J = 12.9 Hz), 144.4, 134.6, 133.1, 122.8, 116.8, 116.2−115.8 (m), 113.0 (d, J = 15.5 Hz), 112.4 (d, J = 3.2 Hz), 112.0, 108.3, 105.1 (t, J = 26.3, 26.3 Hz), 104.6 (t, J = 26.3, 26.3 Hz), 90.2, 84.4, 66.8, 62.0, 60.2, 53.2, 53.2, 50.9. HRMS (ESI-TOF) m/z: [M + Na]$^+$ calcd for $C_{28}H_{24}N_2O_8F_4Na$, 615.1366; found, 615.1360.

4.5. Synthesis of Methyl 5-(2,4-Difluorophenyl)-4-methoxy-1*H*-pyrrole-3-carboxylate 1. Compound **29** (400 g, 1.30 mol) and dimethyl methoxymethylenemalonate **3** (227 g, 1.30 mol) were added to the 5 L reaction flask and dissolved with acetonitrile (2.4 L). Sodium hydroxide (130 g, 3.25 mol) was added in batches, and the mixture was stirred at room temperature for 1 h. After the reaction was completed, sodium hydroxide inorganic base was removed through decompression filtration,[30] ice water (6 L) was added to the mixture and was mechanically stirred for 1 h. Finally, the crude product was obtained by decompression filtration. The intermediate **1** was obtained by reslurry (0.3 L), and rinsing (0.1 L × 2) with ethyl acetate and *n*-heptane (3:15), which was white solid. The product was dissolved in ethyl acetate and then filtered to remove insoluble impurities (298 g, 85.8% yield). HPLC purity: 99.8%. ^{1}H NMR (600 MHz, DMSO-d_6) δ 11.47 (s, 1H), 7.64 (td, J = 8.7, 8.7, 6.6 Hz, 1H), 7.38−7.31 (m, 2H), 7.17 (td, J = 8.7, 8.6, 3.0 Hz, 1H), 3.72 (s, 3H), 3.71 (s, 3H). ^{13}C NMR (151 MHz, DMSO-d_6) δ 163.2, 161.1 (dd, J = 246.8, 12.1 Hz), 158.4 (dd, J = 249.0, 12.2 Hz), 144.2, 130.8 (dd, J = 9.6, 5.0 Hz), 123.0, 115.4 (dd, J = 14.3, 3.8 Hz), 114.0, 111.8 (dd, J = 21.2, 3.5 Hz), 106.9, 104.4 (t, J = 26.3, 26.3 Hz), 61.6, 50.6. HRMS (ESI-TOF) m/z: [M + Na]$^+$ calcd for $C_{13}H_{11}NO_3F_2Na$, 290.0605; found, 290.0605.

■ ASSOCIATED CONTENT

Supporting Information

The Supporting Information is available free of charge at https://pubs.acs.org/doi/10.1021/acsomega.4c04507.

Experimental procedures and characterization data of compounds (NMR, HRMS, DSC-TGA, single-crystal X-ray diffraction, HPLC analysis) (PDF)

■ AUTHOR INFORMATION

Corresponding Authors

Yang Liu − *Key Laboratory of Structure-Based Drug Design & Discovery of Ministry of Education and Key Laboratory of Intelligent Drug Design and New Drug Discovery of Liaoning Province, Shenyang Pharmaceutical University, Shenyang 110016, China;* orcid.org/0000-0002-9284-1944; Email: y.liu@syphu.edu.cn

Maosheng Cheng − *Key Laboratory of Structure-Based Drug Design & Discovery of Ministry of Education and Key Laboratory of Intelligent Drug Design and New Drug Discovery of Liaoning Province, Shenyang Pharmaceutical University, Shenyang 110016, China;* orcid.org/0000-0001-9073-4806; Email: mscheng@syphu.edu.cn

Authors

Ting Wang − *Key Laboratory of Structure-Based Drug Design & Discovery of Ministry of Education and Key Laboratory of Intelligent Drug Design and New Drug Discovery of Liaoning Province, Shenyang Pharmaceutical University, Shenyang 110016, China*

Yueting Hua − *Key Laboratory of Structure-Based Drug Design & Discovery of Ministry of Education and Key Laboratory of Intelligent Drug Design and New Drug Discovery of Liaoning Province, Shenyang Pharmaceutical University, Shenyang 110016, China*

Fangbo Deng − *Key Laboratory of Structure-Based Drug Design & Discovery of Ministry of Education and Key Laboratory of Intelligent Drug Design and New Drug Discovery of Liaoning Province, Shenyang Pharmaceutical University, Shenyang 110016, China*

Rui Wen − *Key Laboratory of Structure-Based Drug Design & Discovery of Ministry of Education and Key Laboratory of Intelligent Drug Design and New Drug Discovery of Liaoning Province, Shenyang Pharmaceutical University, Shenyang 110016, China*

Haoyu Zhang − *Key Laboratory of Structure-Based Drug Design & Discovery of Ministry of Education and Key Laboratory of Intelligent Drug Design and New Drug Discovery of Liaoning Province, Shenyang Pharmaceutical University, Shenyang 110016, China*

Chunshi Li − *Key Laboratory of Structure-Based Drug Design & Discovery of Ministry of Education and Key Laboratory of Intelligent Drug Design and New Drug Discovery of Liaoning Province, Shenyang Pharmaceutical University, Shenyang 110016, China*

Complete contact information is available at: https://pubs.acs.org/10.1021/acsomega.4c04507

Notes

The authors declare no competing financial interest.

https://doi.org/10.1021/acsomega.4c04507
ACS Omega 2024, 9, 37942−37952

■ ACKNOWLEDGMENTS

We gratefully acknowledge the Program for the National Natural Science Foundation of China (grant number 22177079).

■ REFERENCES

(1) Sunwoo, J.; Oh, J.; Moon, S. J.; Ji, S. C.; Lee, S. H.; Yu, K. S.; Kim, H. S.; Lee, A.; Jang, I. J. Safety, tolerability, pharmacodynamics and pharmacokinetics of DWP14012, a novel potassium-competitive acid blocker, in healthy male subjects. *Aliment Pharmacol Ther.* **2018**, *48* (2), 206−218.

(2) Jeong, Y. S.; Kim, M. S.; Lee, N.; Lee, A.; Chae, Y. J.; Chung, S. J.; Lee, K. R. Development of Physiologically Based Pharmacokinetic Model for Orally Administered Fexuprazan in Humans. *Pharmaceutics* **2021**, *13* (6), 813.

(3) Lee, K. N.; Lee, O. Y.; Chun, H. J.; Kim, J. I.; Kim, S. K.; Lee, S. W.; Park, K. S.; Lee, K. L.; Choi, S. C.; Jang, J. Y.; Kim, G. H.; Sung, I. K.; Park, M. I.; Kwon, J. G.; Kim, N.; Kim, J. J.; Lee, S. T.; Kim, H. S.; Kim, K. B.; Lee, Y. C.; Choi, M. G.; Lee, J. S.; Jung, H. Y.; Lee, K. J.; Kim, J. H.; Chung, H. Randomized controlled trial to evaluate the efficacy and safety of fexuprazan compared with esomeprazole in erosive esophagitis. *World J. Gastroenterol* **2022**, *28* (44), 6294−6309.

(4) Hwang, J. G.; Jeon, I.; Park, S. A.; Lee, A.; Yu, K. S.; Jang, I. J.; Lee, S. Pharmacodynamics and pharmacokinetics of DWP14012 (fexuprazan) in healthy subjects with different ethnicities. *Aliment Pharmacol Ther.* **2020**, *52* (11−12), 1648−1657.

(5) Lee, C. H.; Lee, S. C.; Lee, Y. I.; Eom, D. K.; Han, M. R.; Koh, E. J. Novel 4-methoxy pyrrole derivatives or salts thereof and pharmaceutical composition comprising the same. WO 2016/175555 [P], 2016.

(6) Shin, J. T.; Son, J. H.; Lee, S. C. Method for preparing intermediate of 4-methoxypyrrole derivative. US 11345660B2 [P], 2022.

(7) Huang, Z.; Zhou, Z.; Ye, W.; Phillis, A. T.; Mi, C.; Yang, M. Method for preparing potassium ion competitive blocker intermediate. WO 2022/051979 A1 [P], 2002.

(8) Feng, Y.; Qian, W.; Dang, J.; Wang, Z.; Xu, Y. Synthesis of a 4-methoxy pyrrole derivative and its method. CN 116693442 A [P], 2023.

(9) Jiang, H.; Fang, Y.; Zhou, J.; Shao, Z. A preparation method for 4-methoxy pyrrole intermediate. CN 109867617 A [P], 2019.

(10) Qiu, F.; Wu, J.; Zhang, Y.; Hu, M.; Yu, Y. One-pot cascade approach to 1,3′-bipyrrole derivatives from trisubstituted olefins with tosylmethyl-isocyanide (TosMIC). *Tetrahedron Lett.* **2012**, *53*, 446−448.

(11) Qiu, F.; Wu, J.; Zhang, Y.; Hu, M.; Yu, F.; Zhang, G.; Yu, Y. A novel synthesis of multisubstituted pyrroles via trisubstituted olefins and tosmic derivatives. *Lett. Org. Chem.* **2012**, *9* (4), 305−308.

(12) Asian, N.; Cebeci, Y. Application of Box−Behnken design and response surface methodology for modeling of some Turkish coals. *Fuel* **2007**, *86* (1/2), 90−97.

(13) Aslani, H.; Nabizadeh, R.; Nasseri, S.; Mesdaghinia, A.; Alimohammadi, M.; Mahvi, A. H.; Rastkari, N.; Nazmara, S. Application of response surface methodology for modeling and optimization of trichloroacetic acid and turbidity removal using potassium ferrate(VI). *Desalin. Water Treatm.: Sci. Eng.* **2016**, *57* (52), 25317−25328.

(14) Bezerra, M. A.; Santelli, R. E.; Oliveira, E. P.; Villar, L. S.; Escaleira, L. A. Response surface methodology (RSM) as a tool for optimization in analytical chemistry. *Talanta* **2008**, *76* (5), 965−977.

(15) Ragonese, R.; Macka, M.; Hughes, J.; Petocz, P. The use of the Box-Behnken experimental design in the optimization and robustness testing of a capillary electrophoresis method for the analysis of ethambutol hydrochloride in a pharmaceutical formulation. *J. Pharm. Biomed Anal.* **2002**, *27* (6), 995−1007.

(16) Kincl, M.; Turk, S.; Vrecer, F. Application of experimental design methodology in development and optimization of drug release method. *Int. J. Pharm.* **2005**, *291* (1−2), 39−49.

(17) Zhang, F. Y.; Zhou, H. Y.; Yuan, J. Q.; Li, Q. H.; Diao, Y. W.; Zhang, L. J.; Sun, X. Y.; Du, L. Optimization of Nitrosation Reaction for Synthesis of 4-Aminoantipyrine by Response Surface Methodology and Its Reaction Mechanism. *Org. Process Res. Dev.* **2022**, *26* (11), 3051−3066.

(18) Neethu, B.; Tholia, V.; Ghangrekar, M. M. Optimizing performance of a microbial carbon-capture cell using Box-Behnken design. *Process Biochem.* **2020**, *95*, 99−107.

(19) Agbovi, H. K.; Wilson, L. D. Flocculation Optimization of Orthophosphate with FeCl3 and Alginate Using the Box-Behnken Response Surface Methodology. *Ind. Eng. Chem. Res.* **2017**, *56* (12), 3145−3155.

(20) Yuan, Y.; Zhang, Y.; Liu, T.; Hu, P.; Zheng, Q. Optimization of microwave roasting-acid leaching process for vanadium extraction from shale via response surface methodology. *J. Cleaner Prod.* **2019**, *234*, 494−502.

(21) Zhang, R.; Liu, T.; Zhang, Y.; Cai, Z.; Yuan, Y. Preparation of spent fluid catalytic cracking catalyst-metakaolin based geopolymer and its process optimization through response surface method. *Constr. Build. Mater.* **2020**, *264*, No. 120727.

(22) Ranic, M.; Nikolic, M.; Pavlovic, M.; Buntic, A.; Siler-Marinkovic, S.; Dimitrijevic-Brankovic, S. Optimization of microwave-assisted extraction of natural antioxidants from spent espresso coffee grounds by response surface methodology. *J. Cleaner Prod.* **2014**, *80*, 69−79.

(23) Ahmadi, M.; Vahabzadeh, F.; Bonakdarpour, B.; Mofarrah, E.; Mehranian, M. Application of the central composite design and response surface methodology to the advanced treatment of olive oil processing wastewater using Fenton's peroxidation. *J. Hazard Mater.* **2005**, *123* (1−3), 187−195.

(24) Zhang, D. H.; Zhang, J. Y.; Che, W. C.; Wang, Y. A new approach to synthesis of benzyl cinnamate: Optimization by response surface methodology. *Food Chem.* **2016**, *206*, 44−49.

(25) Chen, S.; Sun, S.; Zhao, C.; Zang, M.; Wang, Q.; Liu, Q.; Li, L. Optimization of biodegradation of polycyclic aromatic sulfur heterocycles in soil using response surface methodology. *Pet. Sci. Technol.* **2018**, *36*, 1883−1890.

(26) Sisko, J.; Mellinger, M.; Sheldrake, P. W.; Baine, N. H. α-Tosylbenzyl Isocyanide. In *Organic Syntheses*; 2003; pp 198−198.

(27) Schumacher, C.; Molitor, C.; Smid, S.; Truong, K.-N.; Rissanen, K.; Bolm, C. Mechanochemical Syntheses of N-Containing Heterocycles with TosMIC. *Journal of Organic Chemistry* **2021**, *86* (20), 14213−14222.

(28) Abozeid, M. A.; Kim, H. Y.; Oh, K. Silver-Catalyzed Asymmetric Desymmetrization of Cyclohexadienones via Van Leusen Pyrrole Synthesis. *Org. Lett.* **2022**, *24* (9), 1812−1816.

(29) Xie, R.; Li, R.; Zhao, Q.; Zhao, Y.; Yao, J.; Miao, M. Modular Synthesis of Tetrasubstituted Pyrroles via an Annulative Migration Reaction of Allenyl Ketones and p-Toluenesulfonylmethyl Isocyanide. *Journal of Organic Chemistry* **2023**, *88* (7), 4778−4789.

(30) Wang, Z.; Richter, S. M.; Rozema, M. J.; Schellinger, A.; Smith, K.; Napolitano, J. G. Potential Safety Hazards Associated with Using Acetonitrile and a Strong Aqueous Base. *Org. Process Res. Dev.* **2017**, *21* (10), 1501−1508.

https://doi.org/10.1021/acsomega.4c04507
ACS Omega 2024, 9, 37942−37952